Proceedings of ERAD (2002): 238–242 © Copernicus GmbH 2002

ERAD 2002

Rainfall rate estimate from the rain profiling algorithm "ZPHI" applied to X-band polarimetric radar data

E. Le Bouar[1], **J. Testud**[1], **and S. Y. Matrosov**[2]

[1]Centre d'étude des Environnements Terrestre et Planétaires, Vélizy, France
[2]Cooperative Institute in Environmental Sciences University of Colorado and NOAA ETL, Boulder, USA

Abstract. With dual polarisation capabilities, low-cost X-band radars regain their initial interest associated with a small antenna size for a given angular resolution. To obtain such improvement in correct operational conditions for hydrological applications, the association of this technique with algorithm ZPHI is proposed. Indeed, besides its capabilities to solve the three major causes of uncertainty in the rainfall rate estimate (along-path attenuation; variability of the raindrop size distribution; and radar calibration) ZPHI admits a short radar dwell time, authorising fast scanning velocities. This algorithm has been validated with C-band radar data, through comparisons with ground measurements given by rain gauge and disdrometers.

Very first results of ZPHI applied to X-band radars are presented in this paper. The data are provided by a X-band dual-polarised radar developed and recently upgraded by NOAA/ETL.

1 Introduction

While a number of advantages makes X-band radars appealing for local applications when compared to C- and S-band radars (smaller antenna size, good portability, fine scale resolution, low-cost), propagation effects are stronger. Namely, attenuation is so limiting that it has made X-band radars unsuitable to estimate rainfall rate (R) from reflectivity (Z) measurements only.

Thanks to dual polarisation capabilities, quantitative rainfall rate estimate is possible, by taking advantage of the specific differential phase shift K_{DP}. Several reasons make this parameter particularly eligible for X-band radar:

(i) it is insensitive to attenuation;

(ii) it is insensitive to calibration error;

(iii) it is inversely proportional to wavelength, so that its magnitude is higher than in C- and S-band, and then more usable for light rain;

(iv) the K_{DP}-R transform is quite less sensitive to N_0 variations than Z–R one.

Correspondence to: erwan.lebouar@cetp.ipsl.fr

Additionally, some multi-parameter estimates using K_{DP} have been proposed to completely remove the latter N_0 sensitivity (e.g. Matrosov et al., 2002). However, K_{DP} has to be derived from Φ_{DP}, but estimating it is uneasy in practice because of random phases errors. Unless operating with sufficiently long dwell time, that would be unsatisfactory for operational use, conventional solutions consist of involving a certain range interval for smoothed or weighted finite difference, or for slope estimate by regression approach. Anyway, such an estimate alters the spatial resolution.

Moreover, X-band may suffer the backscatter effect δ contributing to Φ_{DP}, so K_{DP} estimation may be strongly biased if it is not preliminarily removed.

Alternatively, using the rain profiling algorithm ZPHI to derive K_{DP} and then R is proposed in this paper. Indeed, besides its ability to solve the three major causes of uncertainty in the rainfall rate estimate (i.e. along-path attenuation; variability of the raindrop size distribution; and radar calibration) ZPHI admits a short radar dwell time, authorising fast scanning velocities.

While some validation of ZPHI has ever been performed with C-band radar data through comparisons with raingauge and disdrometers measurements (Le Bouar et al., 2001), this paper focuses on a very first application of ZPHI to X-band. The measurements used come from "Hydro" (NOAA/ETL), a recently upgraded dual- polarized X-band radar, and equipped with K_{DP} capability (Martner et al., 2001). Table 1 gives some of its basic characteristics. The dataset illustrating this paper were measured from the Wallops Islands (37.86°N, 75.5°W) on 11 April 2001 at 03:30 UTC.

2 ZPHI algorithm

Algorithm ZPHI (Testud et al., 2000) has been specially developed for dual-polarized radars in attenuating frequencies. It is a profiling algorithm that uses the profile of measured

Table 1.

Hydro characteristics	
Antenna size	3.1 m
Beam width	0.9°
Frequency	9.34 GHz
PRF	2000 Hz
Range resolution	7.5 to 150 m
Doppler Capability	Yes

reflectivity, and a constraint based on $\Delta\Phi$, difference of Φ_{DP} measurements between two selected range bounds. The basic hypothesis assumes that N_0* (intercept parameter of drop size distribution) is constant between these two bounds. This hypothesis is reasonable when the interval is covering an unique kind of rain. Consequently, ZPHI operates a systematic segmentation along each beam, in order to ensure an optimal variability of N_0*, constant in each interval, but variable along the segmented beam.

The primary output parameters are the specific attenuation A (in dB km^{-1}) and N_0* (in m^{-4}). The rainfall rate R is deduced in the following way:

$$R = p\, N_0^{*(1-q)}\, A^q\,, \tag{1}$$

where p and q are coefficients depending on temperature and elevation angle. At temperature T = 10°C and at 0° elevation, p = 1.66 and q = 0.756.

Since A and K_{DP} are nearly proportional, ZPHI may be considered as a sophisticated K_{DP} retrieving method, and the resulting R as a R(K_{DP}) estimate. The difference is that K_{DP} is not directly derived from the "local" lot of measured Φ_{DP}, but it is in part deduced from the estimation constraint by $\Delta\Phi$. In addition, ZPHI is capable to correct the differential reflectivity Z_{DR} for attenuation, utilizing a power-law relationship between A_{DP} (specific differential attenuation) and A. A concrete example of ZPHI performance is provided by Fig. 1, in which correction for attenuation applied to Z and contrast between the derived R and the classical one are shown.

3 Qualification of A retrieval

In ZPHI, retrieving the profile of A along the whole range interval [r_a, r_b] requires the measurements of Φ_{DP} at ranges r_a and r_b only. In order to prevent any contamination of δ effect, r_a and r_b are selected where [$\delta(r_b) - \delta(r_a)$] is suspected to be negligible.

Owing to the A–K_{DP} relationship, Φ_{DP} can be reconstructed in [r_a, r_b] (see Fig. 1b). Two forms of Φ_{DP}, almost independent of each other, are then obtained: one is directly provided by measurements ($\Phi_{DP_{mes}}$), and the other is deduced from a retrieved parameter ($\Phi_{DP_{est}}$).

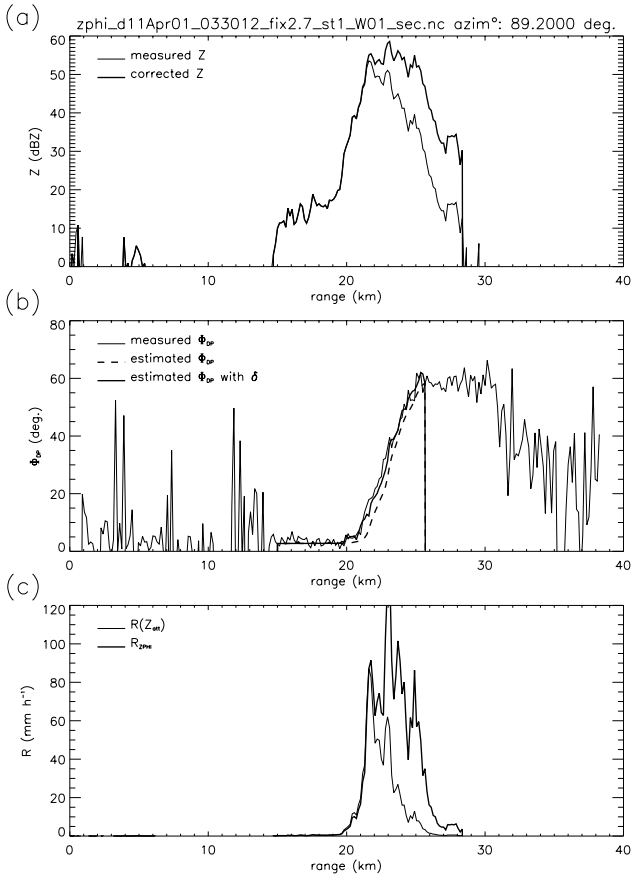

Fig. 1. Profiles along a radar beam. **(a)** Measured reflectivity (thin line) and corrected one (bold line). **(b)** Measured differential phase shift $\Phi_{DP_{mes}}$ (thin line) and estimated one $\Phi_{DP_{est}}$ without (bold dashed line) and with (full bold line) modelled backscatter effect. **(c)** Rainfall rate derived from ZPHI (bold line) and from a Z-R relationship without correction of attenuation (thin line).

Differences between $\Phi_{DP_{est}}$ and $\Phi_{DP_{mes}}$, besides noise fluctuation, are likely to originate from δ effect. The latter can be estimated a *posteriori* from Z_{DR} corrected for attenuation by ZPHI. Note that in X-band, the increase of δ vs. Z_{DR} (Fig. 2, obtained from a T-matrix scattering model with a mixed oblateness law described in Le Bouar et al. (2001)) is perfectly independent of the DSD, as shown in Fig. 2f of Testud et al. (2000). A roughly estimate of δ from Z_{DR} can be given by the following relation:

$$\delta(Z_{DR}) = \begin{cases} (3.95\, Z_{DR} - 4.76) \text{ for } Z_{DR} & \geq 1.2\,\text{dB} \\ 0 & \text{otherwise} \end{cases} \tag{2}$$

The $\Phi_{DP_{est}}$ including the resulting δ is quite consistent with $\Phi_{DP_{mes}}$. This comparison is generalized by Fig. 3, that extends it over a whole sweep. The slope of the resulting linear fit approaches unity (0.99 with δ against 0.88 without δ).

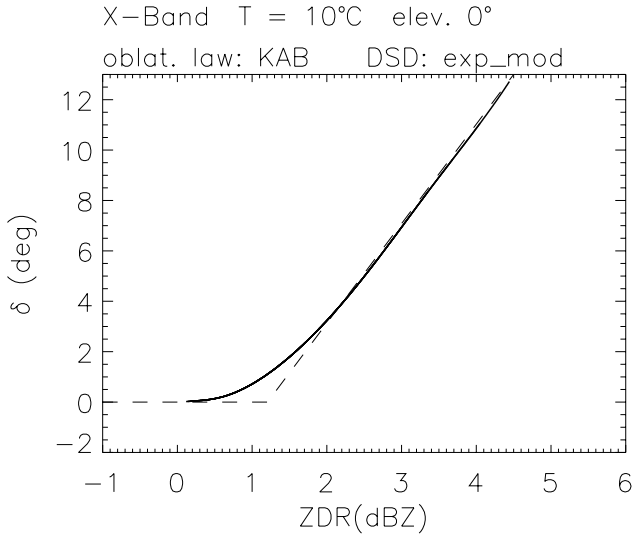

Fig. 2. Backscatter effect δ (in degrees) against Z_{DR} (in dB), simulated by a T-matrix scattering model. Dashed lines stands for the approximation used in this paper.

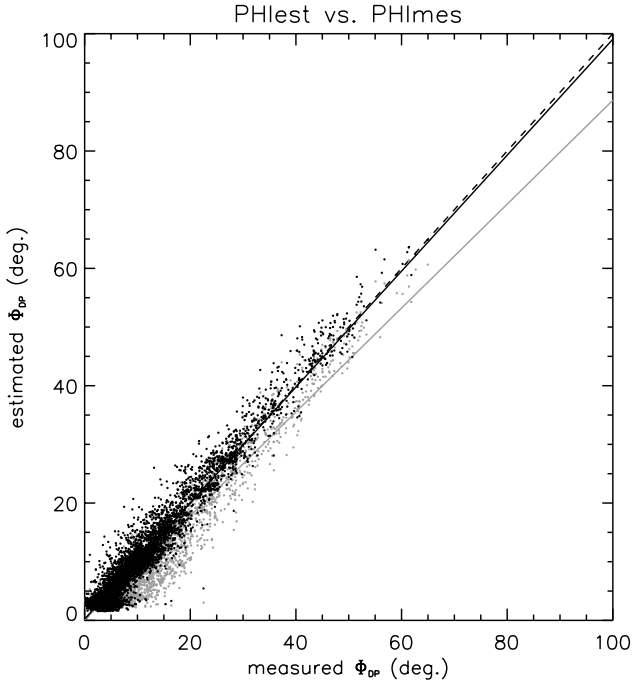

Fig. 3. Scatter plots of $\Phi_{DP_{est}}$ without δ against $\Phi_{DP_{mes}}$ (in grey), and of $\Phi_{DP_{est}}$ with δ against $\Phi_{DP_{mes}}$ (in black). The dashed line refers to the pure unity slope, while the full lines are the linear fit for each scatter plot. In the grey case, the linear Pearson correlation coefficient is 0.942 while in the black case it is 0.963.

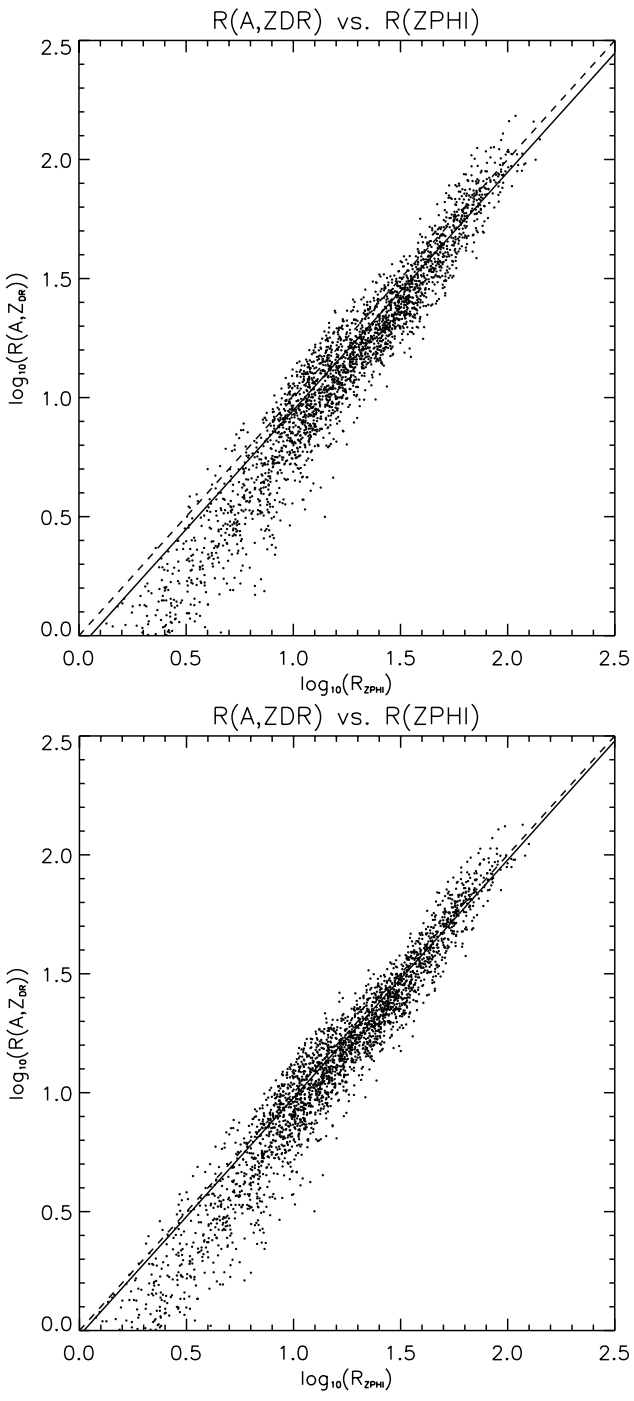

Fig. 4. Scatter plots of $R(A,Z_{DR})$ against R_{ZPHI} before (left panel) and after (right panel) applying a 0.8 dBZ calibration correction. The full lines are determined by the slope of $R(A,Z_{DR})/R_{ZPHI}$ obtained by mean least square.

4 Derived rainfall rate and its dependency on N_0*

One advantage of choosing A or K_{DP} to deduce R lies in their insensitivity to attenuation. However, estimating R from these two parameters necessarily remains subject to N_0* variations, though less than by using some R-Z relationship. By applying ZPHI to data from the BMRC C-band radar at Darwin (Australia), and comparing the deduced R to rain gauge measurements, it was found in Le Bouar et al. (2001) that when attenuation effects had been avoided, a 30% error remained in R when N_0* variations were not considered. In X-band, this error would have been of the same

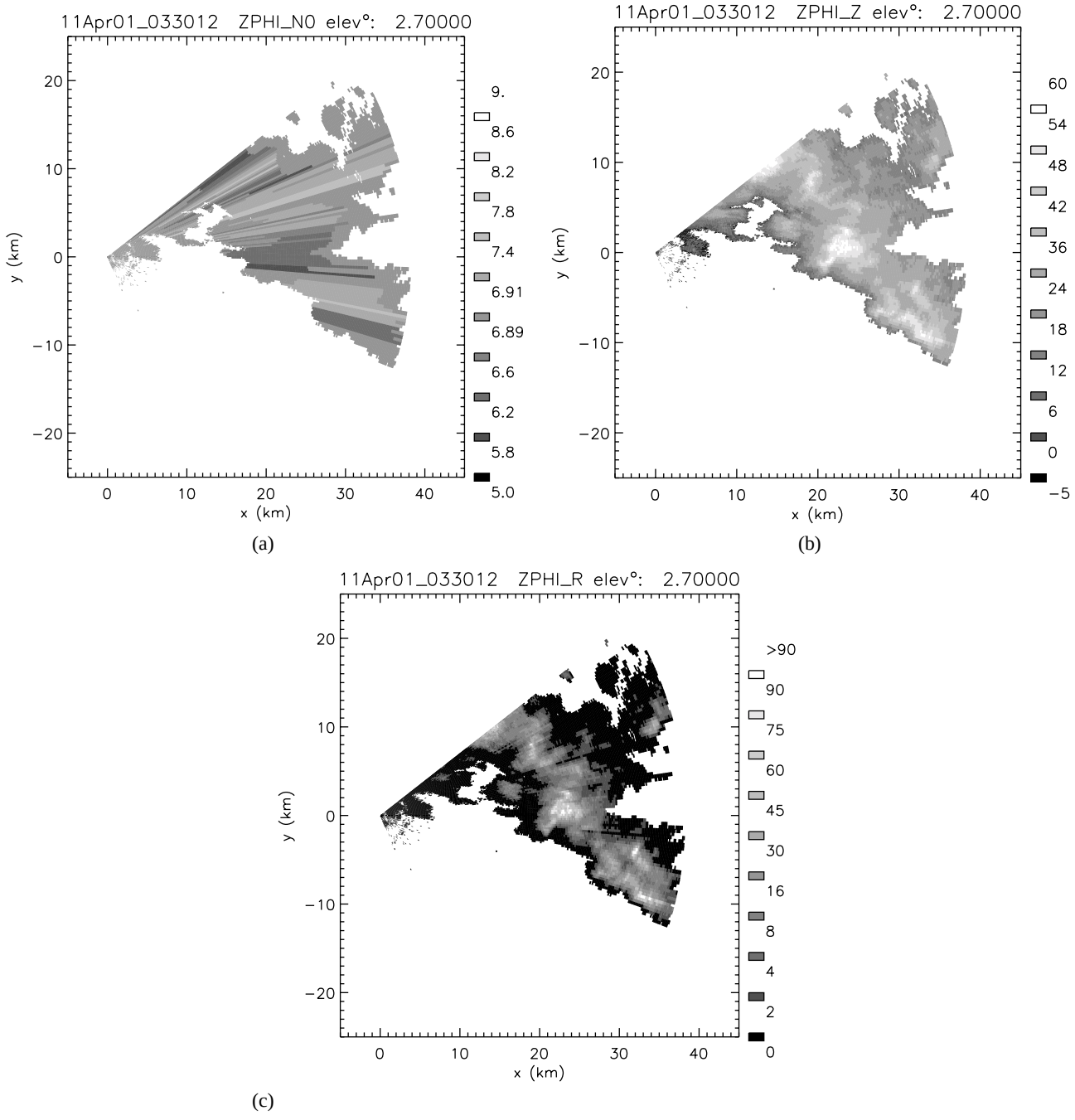

Fig. 5. Hydro PPI views at 2.7° elevation, 11 Apr 2001 at 03:30 UTC. **(a)** decimal logarithm of N_0* being in m^{-4}; **(b)** reflectivity factor corrected for attenuation, in dBZ; **(c)** rainfall rate derived from ZPHI, in mm h^{-1}.

order.

More generally, a 3 dB variation of N_0* leads to some 15% variation for X-band R(A) or R(K_{DP}) estimates.

5 Calibration error

In ZPHI, N_0* is determined through an A-Z power-law expressed as $[A/N_0{*}] = a\,[Z/N_0{*}]^b$. From the latter relation, it follows that if a calibration error C (in dBZ) affects Z, the subsequent error factor in N_0* is $10^{-0.1\,\mathrm{Cb}/(1-\mathrm{b})}$. The impact of C in R estimated by ZPHI (hereafter noted R_{ZPHI}) is a factor error of $10^{-0.1\,\mathrm{Cb}(1-\mathrm{q})/(1-\mathrm{b})}$). With b = 0.756 and q = 0.785, these factor errors are $10^{-0.31\,\mathrm{C}}$ for N_0*, and $10^{-0.067\,\mathrm{C}}$ for R.

As described in Le Bouar et al. (2001), such calibration error may be internally corrected by comparing R_{ZPHI} with an alternate estimate R(A,Z_{DR}) that combines A and the corrected Z_{DR}. Because of attenuation correction, the determination of Z_{DR} depends on calibration error in a complex way

due to the fact that A_{DP} itself depends on N_0*. Nevertheless, retaining only points measurements where differential path attenuation is relatively weak (e.g. close enough to the radar), makes calibration error influence negligible on R(A, Z_{DR}).

So, admitting that R(A,Z_{DR}) = R and R_{ZPHI} = R $10^{-0.067}$ C, C can be found as below:

$$C = 10\,(1-b)/[b(1-q)]\log_{10}[R(A,Z_{DR})/R_{ZPHI}] \quad (3)$$

This expression can be used as a first guess in an iterative procedure when the differential integrated path attenuation is not so negligible. Figure 4 shows a log-log plot of R(A,Z_{DR}) against R_{ZPHI}. The [R(A,Z_{DR})/R_{ZPHI}] slope obtained by least square method is 0.885 (corresponding to a vertical shift of 0.053 in the plot). From this value, the calibration error is found to be 0.8 dBZ. When correcting this error, the resulting slope becomes 0.953.

6 Results on a particular PPI

Figure 5a shows the relatively wide variability of N_0*. Areas where $\log_{10}(N_0*)$ = 6.9 stand for ray segments whose $\Delta\Phi$ is lower than the threshold required for running ZPHI: in this case, N_0* is forced to an arbitrary value (here, Marshall Palmer's one). This imposed value explains some ray-to-ray contrast in the derived R sweep in Fig. 5(c).

Surprisingly, weak N_0* from $10^{5.9}$ to $10^{6.4}\,m^{-4}$ are observed where reflectivity ranges from 50 to 60 dBZ, whereas N_0* values higher than Marshall Palmer's are observed for lower reflectivities (see Fig. 5b vs. Fig. 5a). Such weakness of N_0* associated with strong Z could be attributed to the presence of hail: because it tends to enhance reflectivity and has a reduced effect on Φ_{DP}, it could explain some underestimation of N_0* in ZPHI. However, the cores of strong Z are associated with $Z_{DR} > 3$ dB (not shown), suggesting that they are presumably of heavy rain nature, with relatively large raindrops. In a sense, this is quite consistent with low N_0*, since N_0* is inversely proportional to the power 4 of the mean volume raindrop diameter.

In addition, self-consistent scatter plots like those of Fig. 3 or Fig. 4 support the assessment that only pure rain is present.

7 Summary and conclusions

Several reasons make ZPHI particularly designed for X-band, at which both propagation and backscatter effects are strong when compared to C- and S-bands: Not only it corrects for attenuation, but also it systematically removes backscatter effects, provided the bounds of the treatment, i.e. r_a and r_b, are properly selected. Despite the unavailability of collocated validation data like disdrometer or rain gauge ones, self-consistent validation procedures have allowed some validation of ZPHI. For one, systematic comparisons between measured and derived Φ_{DP} constitute a self-quality control for the retrieval of the specific attenuation A. For this purpose, modelling parameter δ turns out to be necessary. For another, comparison between R derived from ZPHI and R(A,Z_{DR}) may control the retrieved N_0*, sensitive to radar calibration errors. Obviously, self consistency is reached out only if applied to rain data. For this reason, these control procedures may constitute a tool for detecting some non rain hydrometeors like hail.

Furthermore, ZPHI automatically adjusts the R-A relationship through the matching of N_0*. This aspect is of major importance, particularly in some situations like the one illustrated by Fig. 5, characterized by a large variability of N_0*.

Acknowledgement. The authors wish to acknowledge NOAA/ETL for providing their Hydro X-band radar data.

References

Le Bouar, E., J. Testud, and T. D. Keenan, 2001 : Validation of the rain profiling algorithm "ZPHI" from the C-band polarimetric weather radar in Darwin. J. Atmos. Oceanic Technol., 18, 1819-1837.

Martner, B. E., K. A. Clark, S. Y. Matrosov, W. C. Campbell, and J. S. Gibson, 2001: NOAA/ETL's polarization-upgraded X-band "Hydro" radar. Preprints, 30th Intl. Conf. On Radar Meteor., Munich, Germany, 101-103.

Matrosov, S. Y., Clark, K. A., and Martner, B. E., 2002: X-band polarimetric radar measurements of rainfall. J. Appl. Meteor., 41, 941–952.

Testud, J., Le Bouar, E., Obligis, E., and Ali-Mehenni, M., 2000: The rain profiling algorithm applied to polarimetric weather radar. J. Atmos. Oceanic Technol., 17, 332-356.